ELSEVIER

International Journal of Coal Geology 49 (2002) 195–214

International Journal of COAL GEOLOGY

www.elsevier.com/locate/ijcoalgeo

Relationship between in situ coal stratigraphy and particle size and composition after breakage in bituminous coals

J.S. Esterle [a,*], Y. Kolatschek [b], G. O'Brien [a]

[a] *Queensland Center for Advanced Technologies, CSIRO Exploration and Mining, PO Box 883, Kenmore, Qld 4069, Australia*
[b] *Julius Kruttschnitt Minerals Research Centre, Indooroopilly, Qld 4068, Australia*

Received 21 March 2001; received in revised form 19 July 2001; accepted 1 October 2001

Abstract

The hypothesis that the parent stratigraphy of a coal seam, i.e. its lithotype and band distribution, can be used to estimate the input and output size distributions of broken coal for a fragmentation event(s) was tested using the drop-shatter process for core. Coal breakage is a function of the inherent strength of the material, its particle size, and the amount of impact energy imparted. Coal is composed of a heterogeneous mixture of bright and dull bands, and stone, which generate different daughter particle size distributions in response to impact energy. Lithotypes and bands also exhibit an in situ thickness distribution that can be related to input and output size distributions. The results demonstrate that dull coal that is massive and strong requires more energy to break relative to brighter, more friable coals. As a result, brighter and banded coal lithotypes break into finer band components, resulting in the concentration of bright (vitrinite-rich) coal in the finer progeny fractions. Dull coal and stone concentrate in the coarse fractions, except where stone consists of soft claystones or shales. The frequency distributions of the lithotypes' thickness estimate the feed size, and that of the component bright, dull and stone bands of the daughter particle size distribution at the end of the fragmentation process. This has implications for the prediction of size, and composition of size fractions, resulting from fragmentation events that occur during mining and handling, both of which will impact on the downstream processing behaviour of coal.

Keywords: Fragmentation; Particle size prediction; Lithotypes; Coal texture; Drop-shatter testing

1. Introduction

Accurate prediction of coal breakage and resulting daughter particle size distribution is critical to the efficient design and operation of coal processing plants. Intact coal seams break down into variously sized particles as coal is mined and transported to the plant. The amount of size degradation depends on the cumulative breakage energy imparted to the coal and on the inherent strength of the coal. Although the bulk material strength of coal is dependent upon its rank and composition, the relative strengths of individual coal particles is also dependent upon their size. For all materials, the energy required for size reduction is proportional to the new surface area created; hence, more energy is required for a smaller parent to achieve an equivalent amount of breakage to a larger parent

* Corresponding author. Tel.: +61-7-3327-4411; fax: +61-7-3327-4455.
E-mail address: joan.esterle@csiro.au (J.S. Esterle).

0166-5162/02/$ - see front matter
PII: S0166-5162(01)00077-5

(Rittinger, 1867). With coal, this behaviour is compounded by the fact that smaller particles contain fewer inherent fractures or cleat and this applies to both dull (durain) and bright (vitrain) lithotypes (Esterle et al., 1994).

Coal is composed of a heterogeneous mixture of bright and dull bands and stone, each of which has different strength, fracture density, thickness, and microscopic composition. The fractures, and the boundaries between and within lithotypes and stone, form planes of weakness that will promote separation of components during the breakage process. Hence, the parent coal lithotype stratigraphy should provide an estimate of the in situ size distribution and composition of feed entering the breakage process. At some energy, the individual band components should start to liberate from the parent lithotypes. Therefore, the stratigraphy of bright and dull bands comprising the lithotypes should provide an estimate of the size and composition of the liberated daughter particles at the end of the process. This hypothesis was a favorite of John Ferm (personal communication), and it is tested in this study.

2. Background

Coal is a banded material and its strength properties vary as a function of rank, composition, and texture. At a megascopic scale, coal seams can be subdivided into layers or lithotypes (Stopes, 1919) that are classified by the proportion of bright vitrain bands in an attrital matrix. The attrital matrix can appear dull or bright depending on its composition (Schopf, 1960). The massive appearance of attrital matrix is a function of its microscopic size distribution and this contributes to its strength relative to banded lithotypes. A variety of field classification systems exist for coal and each estimates the proportion of bright bands to matrix along a transect from the top to bottom of a seam. Although not commonly analyzed as such, the thickness distribution of lithotypes, or their component bands, can be used as a measure of coal mass texture for a given coal seam.

Moore and Ferm (1988, 1992) quantified coal mass texture using the thickness distribution of vitrain bands in Indonesian coals. They found that megascopic vitrain bands exhibited size frequency modes around 3–4 phi, or 1.3–0.3 mm, and attributed this to the degree of degradation, and the plant communities that formed the paleo-peat. Among coal lithotypes with similarly high vitrinite content, they found differences in grindability between banded and nonbanded-bright coals, and between thinly and thickly banded-bright coals. Hower (1998), among others, also demonstrated that different lithotypes have different grindability for Carboniferous-age coals. A number of other studies have examined changes in vitrain band size and abundance within and between coals of different ages to determine changes in paleo-botanical assemblages, as well as environments of deposition (Moore and Hilbert, 1992; Shearer and Moore, 1994a,b; Shearer et al., 1995; Ward et al., 1995). Wang et al. (1996) progressed the analysis of coal mass texture a step further and found that different lithotypes, in addition to component vitrain bands, exhibited different size frequency modes for Carboniferous-age coals. In general, the frequency mode for all lithotypes was at 64 + 32 mm. Pure vitrain bands exhibited a mode at 8 + 4 mm, whereas the durains exhibited a mode at 64 + 32 mm. These modes were also shown to vary with differing depositional environments. Previously, Hunt (1988) suggested that lithotype thickness distributions provide an estimate of basin subsidence and sedimentation rates.

The above studies provoked some discussion about coal texture, but the application of its measurement to predicting breakage and daughter particle size distribution was not tested. Esterle et al. (1994) examined the differing breakage properties of coal lithotypes in Permian age seams at low energies experienced during mining and crushing. They were also able to estimate a mean block size obtained by analyzing the volume distribution of lithotypes within a seam as an input to blast fragmentation models (Esterle et al., 2000a). The latter provided a capability to design a blast for controlled fragmentation as well as liberation of stone from coal.

Coal breakage is not only related to the inherent friability of a coal seam. Regardless of method (compression, impact, shear), increased force or energy will increase the amount of damage, resulting in fragmentation of a material. This has been demonstrated for relatively low-energy breakage events during the mine extraction and handling chain (Esterle et al., 2000b), and for higher energy grinding (Bailey

and Esterle, 1996). During coal blasting, excessive damage occurs in the high-energy crushing zone around the charge in the drill hole. However, blast energy declines away from the charge and fragmentation occurs through radial cracking within approximately 3 m of the hole. Fragmentation through the rest of the block occurs through the propagation of gases and pressure through the inherent flaws (joints, lithotype bedding and cleat) within the coal mass structure. Hence, the majority of the fragmentation, after dislodging the coal, will take place during the excavation and loading, and these are lower energy events (Esterle et al., 2000a).

The energy required for size reduction is proportional to the new surface area created; hence, more energy is required for a smaller parent to achieve an equivalent amount of breakage when compared to a larger parent (Rittinger, 1867). During the breakage process, a melange of coal particles with different (and changing) parent size and composition behave as interacting, but independent, entities as they undergo damage and size reduction.

Studies by Swanson et al. (1993) suggested that the rate of size degradation varies during breakage. During the drop-shatter process, most Australian, Permian-age coals exhibit a rapid breakage rate up to 4 or 6 drops, thereafter declining out to 14 or so drops where the rate slows again. They attributed this rate change, often described colloquially as a ''fatal'' or ''stabilized'' size distribution, to the geologic character of the coal seam, i.e. its petrographic composition, texture and cleat density.

Against this background, we examined the degree to which the parent stratigraphy of a coal seam could be used to estimate the resulting size distribution and lithotype composition of liberated daughter particles after a given breakage event. The drop-shatter test was used as the breakage event. The experiment was designed to measure and examine the relationships between the:

- in situ size and composition estimated by lithotypes and component bands in intact core;
- size and composition of daughter particles after the core had been dropped to a stable size distribution; and
- energy required to break plies and lithotypes to a stable size distribution.

3. Methods

The experiment was conducted on bore core extracted from a mining block in a Permian age coal seam in the Bowen Basin. A 100 mm core was extracted for drop-shatter testing and daughter particle analysis (Kolatschek, 2000). Standard lithotype profiling was conducted on this, and higher resolution band profiling on an adjacent 200 mm large diameter core collected 1 m away. Other samples were collected from the exposed face of the mining block for single-particle breakage testing of individual lithotypes, and to examine the conditioning effect of successive breakage events.

The studied seam is 7.6 m thick at the sampling location and it consists pervasively of a banded-bright base that is overlain by duller lithotypes with abundant stone partings and grades upward into a variably banded top. The rank of the seam is mid-volatile bituminous with a vitrinite reflectance of $R_{vmax} = 1.2\%$.

3.1. Megascopic profiling and size classification of intact core

In the field, the core was profiled at two resolutions: lithotype and band. Lithotypes were first proposed by Stopes (1919) to describe the ''four visible ingredients'' in banded bituminous coals. Lithotypes can be thought of as sedimentary beds consisting predominantly of two components, bright and dull layers, in varying proportions. These beds can contain minor amounts of fusain and/or stone, which are described separately. Cleat spacing was not quantified, but appeared to vary from 1 to 10 mm in the bright bands to 10 to 30 mm in the dull bands.

In this study, lithotype profiling followed the Standards Australian AS2519-1993 (Standards Association of Australia, 1993) using a minimum thickness of 5 mm for distinction (see Table 1). Band profiling followed a modified version of Moore and Ferm (1992) using a minimum band thickness of 1 mm and classifying bands into discrete components, bright or dull. In some cases, particularly in banded-bright lithotypes, bands were visible, but less than or equal to 1 mm and tightly packed. Here, a default banded-bright was used at the band level, and the interval subdivided into 1 mm increments of equal cumulative

Table 1
Correlation between terms for megascopic description of banded coal (after Stopes, 1919; Diessel, 1965)

Stopes' lithotypes (1919)	Australian Standard lithotypes, 5 mm resolution (abbreviations in this paper)	Proportion of bright bands (%)	Band profiling, 1 mm resolution
Vitrain	Bright (Brt)	>90	Bright (Brt)
Clarain	Banded-bright coal (BB)	60–90	
"Duro-clarain"	Inter-banded coal (IB)	40–60	
"Claro-durain"	Banded dull coal (DB)	10–40	
Durain	Dull coal w/Minor Bright (DM)	1–10	
Durain	Dull coal (D)	<1	Dull (D)
Fusain	Fibrous coal (F)		

Stone is not included in this classification.

length. At both resolutions, stone bands were measured separately.

The lithotype and band data were analysed to obtain volumetric proportions and frequency distributions by thickness for plies and for the total seam. Relative linear proportions for the total seam were determined by summing the cumulative thickness of each lithotype or band across the total length of the core. Assuming constant lithotype thickness across the core, the linear proportion can be considered equal to volume. Linear proportions within a thickness class were obtained by summing the cumulative thickness of each lithotype or band within a given thickness class. Relative densities (density bottle method AS1039.21.1,1-1994, Standards Association of Australia, 1994) were measured for different lithotypes occurring in the drop-shatter progeny and used to calculate a mass distribution of lithotypes by thickness class. Thickness classes were comparable to "percent retained" for a root 2 sieve series (i.e. >= 0.5, 1, 2, 4, 8 mm, etc).

Following Ferm's previous studies, the lithotype and band data were also analysed to obtain a thickness frequency distribution (Moore and Ferm, 1988; Wang et al., 1996). Both types of distributions, volume and frequency, were used to compare between the thickness distribution of lithotypes and bands in situ and the size distribution and composition of daughter particles *after fragmentation* during drop-shatter.

3.2. Bore core drop-shatter testing

The 100 mm core was drop-shattered following the modified procedure of Swanson (Swanson et al., 1998, ASTM, 1986). Due to the thickness of the seam, core was subdivided into a series of three plies, each of which showed lateral continuity across the study area. The individual plies were weighed, air-dried, and re-weighed before testing. The samples were repetitively dropped from a height of 2 m onto a steel plate and a size distribution obtained after every second drop (up to and including 14 drops). Core was dropped an additional six times and a final size distribution obtained after 20 drops. This total number of drops is commonly used across the Australian coal industry to approach, as near as practical, a stabilized size distribution.

3.3. Daughter particle analysis

The sized daughter particles after 20 drops were analysed for lithotype composition. Samples of different lithotypes in the different size fractions were also analysed for relative density to assist in conversions between mass and volume for comparison between the in situ core and the broken daughter particles.

3.3.1. Sample preparation

Daughter particles from the plies after 20 drops were sieved at 31.5, 16, 8, 4 and 2 mm. All particles in the size fractions larger than 16 mm were classified into lithotypes. The smaller size fractions were split (cone and quartered) into more manageable subsamples, ensuring the presence of at least 500 particles for characterisation. The 2 mm undersize material was rotary divided into subsamples weighing between 1000 and 1200 g. The subsamples were then screened at 1, 0.5, 0.25, 0.125 and 0.063 mm and the resulting size fractions were prepared as polished blocks for microscopic examination.

3.3.2. Macroscopic characterisation of daughter particles >2 mm

The >2 mm progeny was characterised macroscopically under a magnifying glass fitted with a

fluorescent light ring, which ensured constant lighting conditions. Particles were sorted into different lithotype classes according to the Australian Standard terminology used for profiling (Table 1). The number and mass of particles in each lithotype category were recorded for each size class.

3.3.3. Microscopic characterisation of daughter particles <2 mm

The <2 mm progeny was characterised microscopically using a reflected light microscope and a suite of air objectives of 5×, 10× and 20× magnification. In order to establish a microscopic classification system comparable to the macroscopic classification, a duplicate sample of each lithotype in the 4+2 mm fraction was individually set in resin and examined under a reflected light microscope. The proportion of bright to dull in each particle was estimated and particle classified as one of the following:

- bright (B), >90% telovitrinite;
- banded-bright (BB), 60–90% telovitrinite;
- inter-banded (IB), 40–60% telovitrinite;
- dull (D) low minerals, <40% telovitrinite with <20% mineral matter content;
- dull (D) high minerals, <40% telovitrinite with >20% mineral matter content;
- stone, >90% mineral matter.

Bright bands were microscopically represented by telovitrinite. Dull was represented by the matrix macerals, consisting predominantly of the inertinite group macerals (semifusinite and inertodetrinite), with detrovitrinite, mineral matter, and rare liptinite macerals.

3.3.4. Single-particle breakage characterisation

Controlled breakage of single particles was undertaken using a drop weight and drop tower tester. The purpose of the test work was to establish the breakage properties of lithotypes and to determine the effect of particle size and composition on the breakage characteristics. Conditioning of coal types during successive breakage events was also examined. The analysis of the breakage results provides breakage functions that relate the specific comminution energy to the output size distribution from a known parent. These were used by Kolatschek (2000) to mathematically model the process.

The drop weight tester is comprised of a drop weight head mounted on two guide rails that can be lowered or raised to a desired drop height above a steel anvil using an electric winch. The drop weight head is released by a pneumatic switch and falls under gravity onto the test specimen placed on the anvil. The broken fragments are collected and sized. Repeatability on the test is within 2% (Esterle and O'Brien, unpublished data).

Blocks were tested in batches of 30 or more particles, depending on their size and mass. The energy imparted to the particle is determined by the mass of the drop weight head and its height above the particle (Narayanan and Whiten, 1988). The available apparatus was used to test particles down to 8 mm, at energies ranging from 0.01 to 0.15 kW h/t.

A drop-shatter tower was used to test small particles at very low energies of breakage (see Kolatschek, 2000). In this method, particles were dropped from a known height through a pipe onto an impact plate. Three effective drop heights were used: 1, 2 and 3.6 m; equating to approximately 0.0027, 0.0055 and 0.0098 kW h/t, respectively. The lower energies were required to model the range of energies and particle sizes that would participate in the drop-shatter process.

Conditioning of coals during successive breakage was examined by drop-shattering a batch of banded-bright and dull-banded coal repeatedly from a height of 2 m. After each drop, the fraction of material passing one tenth of the original particle size was removed and the oversized dropped again. The size distribution parameter t10 measured after each drop was then plotted against the drop number.

To obtain sufficient lithotype samples for particle breakage testing, particles were collected from the face of the exposed coal block from which the core was extracted. A channel of the complete seam face was excavated and the resulting coal pile was sorted into the following lithotypes for sampling: combined D to DM, DB to IB, and BB. Stone was also collected. Drop weight experiments were conducted on 75×45 mm blocks at high energies; drop tower tests were conducted on a suite of block sizes at lower energies (see Kolatschek, 2000 for details of sampling, sample preparation, and testing apparatuses).

4. Results

4.1. Coal profiles

The lithotype and band profiles are presented in Fig. 1. Both show a similar vertical trend. Although the band profiling did not account for approximately 8% of the total seam thickness, the linear proportion of plies within the core was similar, allowing comparisons to be made for composition and thickness distributions across the total seam.

The seam at the sample location is approximately 7.6 m thick. The base of the seam consists predominantly of low ash yield, banded-bright coal (Ply C).

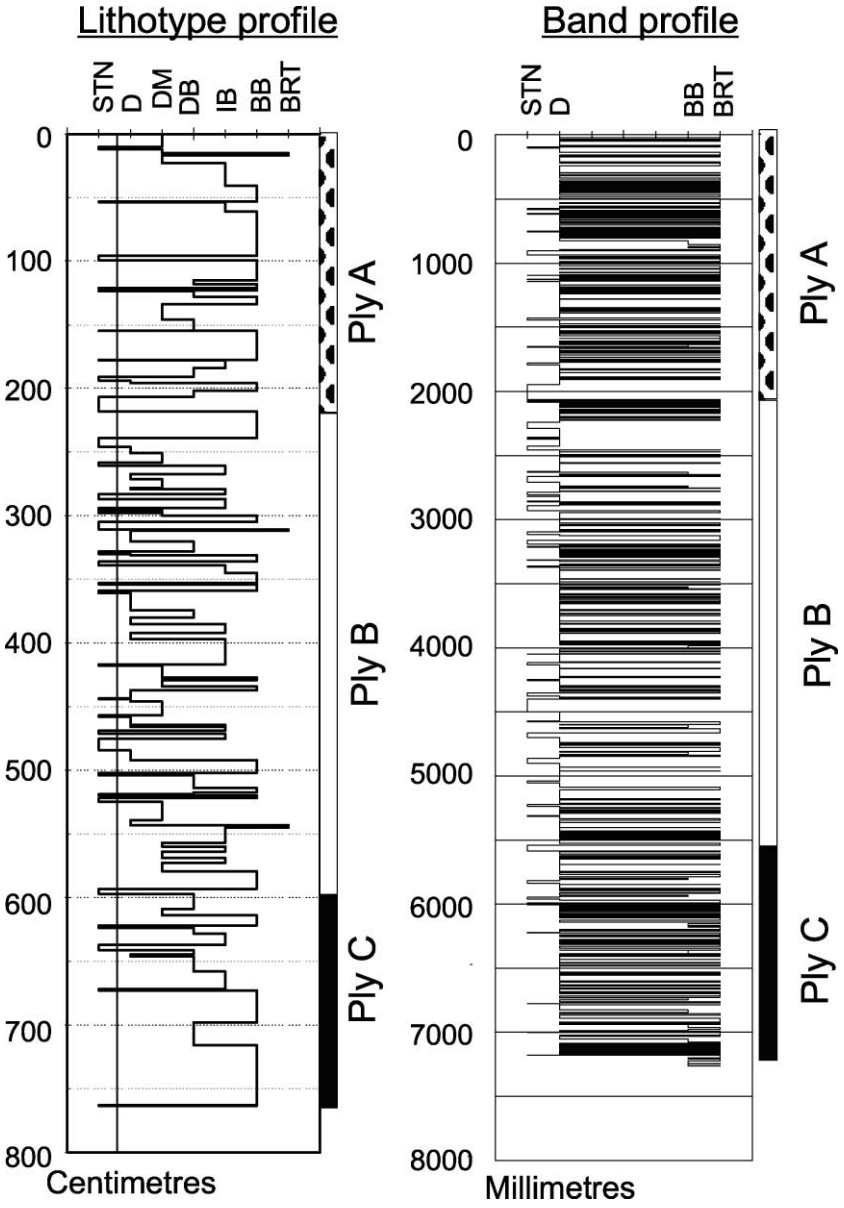

Fig. 1. Lithotype and band profiles for the test core showing the location of the ply samples used for drop-shatter testing. Ply A = 29%, Ply B = 50%, and Ply C = 22% of total seam estimated from length.

This ply is overlain by stone band-rich dull to inter-banded mid-section (Ply B). The seam is capped by an inter-banded to banded-bright coal sequence (Ply A). This ''dulling up'' profile is common to Australian Permian-age coals (Smyth and Cook, 1976). The composition of the plies and total core is presented in Table 2.

Comparison of composition between lithotype and band profiling is in fair agreement, especially for stone. In order to compare between lithotype and band for coal types, the lithotype data were grouped into end-member ''dull coal''=(D + DM + DB + IB) and ''bright coal''=(BB + BRT). By doing so, the proportions of end-member bright coal was around 32.5%, of dull coal 56.9% and of stone 10.6% by volume for the total seam. This matches the band estimation well. These data will be addressed later and compared to the composition of progeny from the drop-shatter testing.

4.2. Thickness distribution of lithotypes and bands

The thickness distribution of the different lithotypes and bands was estimated by frequency and by calculated volume. To be consistent with the field of sedimentary petrology, Moore and Ferm (1992) adopted the size frequency distribution method for analysing coal texture. For comparison to their findings, the lithotype and banding data from our profiles are presented as frequency in Fig. 2.

All lithotypes are normally distributed, with a mode in the 64 + 32 mm size bin (Fig. 2a). This is similar to the mode found for Carboniferous-age coals in the Appalachian basin (Wang et al., 1996). The coarser bins are dominated by the bright category lithotypes banded-bright and inter-banded. The dull category lithotypes and stone dominate the finer bin sizes.

Individual bands exhibit a much finer thickness distribution, with a frequency mode at 8 + 4 mm (Fig. 2b). Stone is widely distributed with respect to size, and the dull and bright to banded-bright units appear of similar size distributions. However, this distribution does not take into account the fact that the banded-bright intervals consisted of tightly packed 1 mm, or less, thick vitrain bands. If these were considered as independent entities, the bright band thickness distribution would become bimodal with a second population consisting predominantly of bright bands in the 2 + 0 mm class (Fig. 2c).

Another method for analysing the in situ size distributions is to calculate the mass percent of lithotypes in each size fraction. Mass was calculated by multiplying the linear proportion of each lithotype in each size fraction by the average measured density of each lithotype. The density values are given in Tables A-1 to A-4 in Appendix A.

As expected, the relative distributions are similar, but shifted into the coarser size classes for both the lithotypes and the bands (Fig. 3). The greatest proportion of lithotypes by mass occurs in the 128 + 64 mm size class. The coarser sizes are still dominated by brighter coal lithotypes, whereas the dull lithotypes and stone occupy the bins between 128 and 4 mm.

Table 2
Linear proportions of lithotypes and bands in core estimated from profiling

R23_100 lithotypes	Stone	D	DM	DB	IB	BB	BRT	Total
Ply A	7.1	0.9	13.1	11.3	29.7	36.4	1.4	100.0
Ply B	15.8	14.5	10.0	24.8	15.7	17.4	1.7	100.0
Ply C	4.1	0.0	8.8	18.1	16.1	52.8	0.0	100.0
Total core	10.6	7.2	10.6	19.5	19.6	31.3	1.2	100.0
R23_LD_bands	Stone	D				BB	BRT	Total
Ply A	10.2	52.3				2.6	34.9	100.0
Ply B	16.1	61.6				2.9	19.4	100.0
Ply C	3.2	48.7				12.4	35.6	100.0
Total core	11.4	55.9				5.0	27.6	100.0
Grouped lithotypes total core	10.6	56.9				32.5		100.00

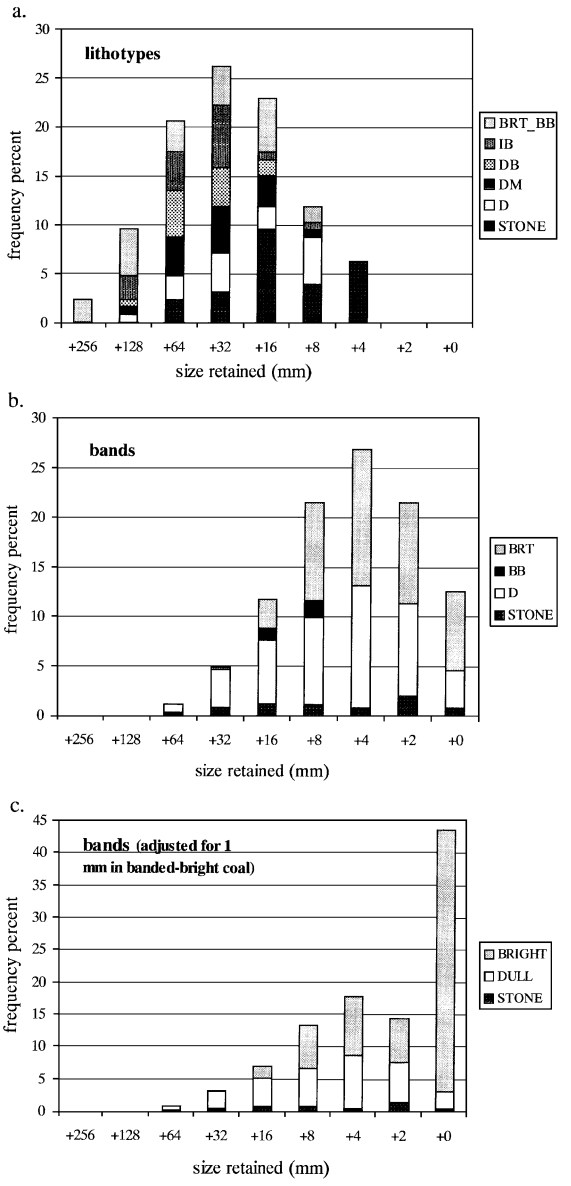

Fig. 2. Size frequency distribution of (a) lithotypes ($n = 126$); (b) bands derived from profiling ($n = 749$); and (c) bands derived from profiling with banded-bright coal adjusted for component 1 mm bands ($n = 1124$).

From the band profile, the stone shows the coarsest distribution, followed by the dull bands in the 64 + 32 mm size class, and the bright bands across the finer sizes.

The rationale behind the size discrimination of end-member "bright" and "dull" bands within the in situ core is that we want to test the hypothesis that the composite lithotypes will break down and eventually liberate their component bands at some energy. However, it is not known which method of size analysis provides a better estimate of the broken daughter particles.

4.3. Breakage behaviour of different lithotypes

The results of the single-particle breakage tests of lithotype samples, presented as a fineness indicator graphed against energy, are given in Fig. 4. Here, the fineness indicator represents the mass percent passing 1/10 of the parent particle top size (termed T10). By using this indicator, one can compare between differ-

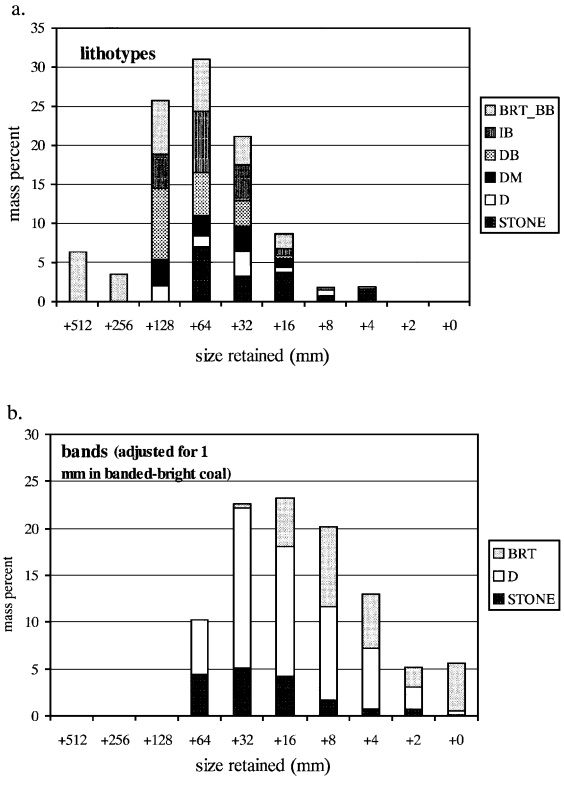

Fig. 3. Calculated mass distribution of lithotypes across size size fractions. (a) Lithotypes. (b) Bands with 1 mm adjustment for banded-bright zones.

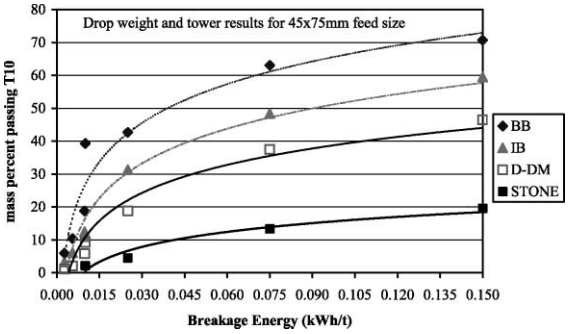

Fig. 4. Increasing breakage with increasing energy for different coal types. Samples from study area in the Bowen Basin. BB = banded-bright, IB = inter-banded; D – DM = dull to dull with minor coal types. Data are from Kolatschek (2000). Abbreviations given in Table 1.

ent block sizes to examine the relative amount of size reduction as a function of energy.

The single-particle tests show that size degradation increases with increasing energy and that rates are initially rapid from 0 to 0.025 kW h/t of energy, thereafter declining. Similar results were seen by Swanson et al. (1993) for drop-shatter tests of coal. As the energy increases, the discrimination of breakage behaviour between different lithotypes increases. At a given energy, say 0.025 kW h/t, banded-bright lithotypes produce around 10% more fine particles than inter-banded lithotypes, and 20% more than dull lithotypes. The corollary to this is that dull coals require substantially more energy to break to a similar daughter particle size to that of bright coals.

In this seam, stone is predominantly a fine-grained, dolomitized tuffaceous siltstone that is substantially harder than the coal in the seam. As a result, rotary breakers prior to processing at the mine site remove much of the stone. These relative differences due to coal type and rock are maintained, regardless of particle size.

Differences in coal strength within a seam have implications for controlling fragmentation, in particular the generation of fines, during blasting (by positioning of the charge), handling (drop heights on transfer points) and crushing (power draw and design). Differences between seams, or the same seam in different mines or pits, can be augmented by a change in rank. Similar trends are observed during the higher energy process of grinding (see extensive review by Hower, 1998).

Parent particle size effect is demonstrated in Fig. 5. The energies shown in this graph are much lower than in the previous data set, but the differences between end-member coal types are still significant, around 10%. In this graph, the fineness indicator T10 changes relative to parent particle size. For example, T10 for 75 + 45 mm particles is 6 mm and for 45 + 31.5 mm it is 3.8 mm, and so on. The significance of this graph is that more energy is required to reduce smaller parent particles to a relative proportion of their top size. This is a demonstration of Rittenger's law, stated previously. Another observation is that the banded-bright coals exhibit a stronger size effect than do the dull coals. This is due to the higher variability in banding and cleat structure in the banded-bright coal relative to the massive dull coal.

The conditioning tests corroborate the behavioural differences described above for both coal type and size (Fig. 6). The fraction of material passing one tenth of the original particle size (t10 parameter) for the banded-bright coal starts at approximately 9% after the first drop and steadily decreases to around 3% after drop 20. The decline in breakage is initially rapid and then begins to slow after about 14 drops. The reduction in the degree of breakage indicates an apparent hardening of the banded-bright coal. This hardening effect can be explained by the rapid consumption of flaws or fractures in the banded-bright

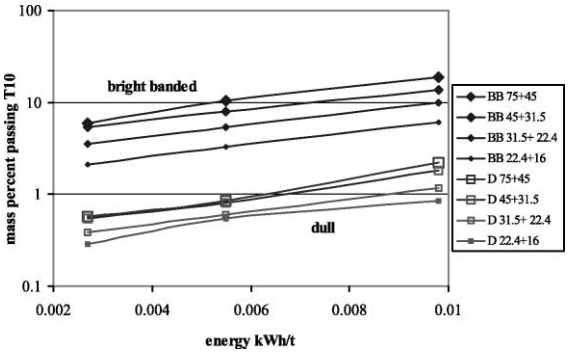

Fig. 5. The effect of particle size on breakage behaviour presented as a graph of T10 against comminution energy. T10 is 1/10 of the average top size of the parent particle. Samples from test seam in the Bowen Basin. Data are from Kolatschek (2000).

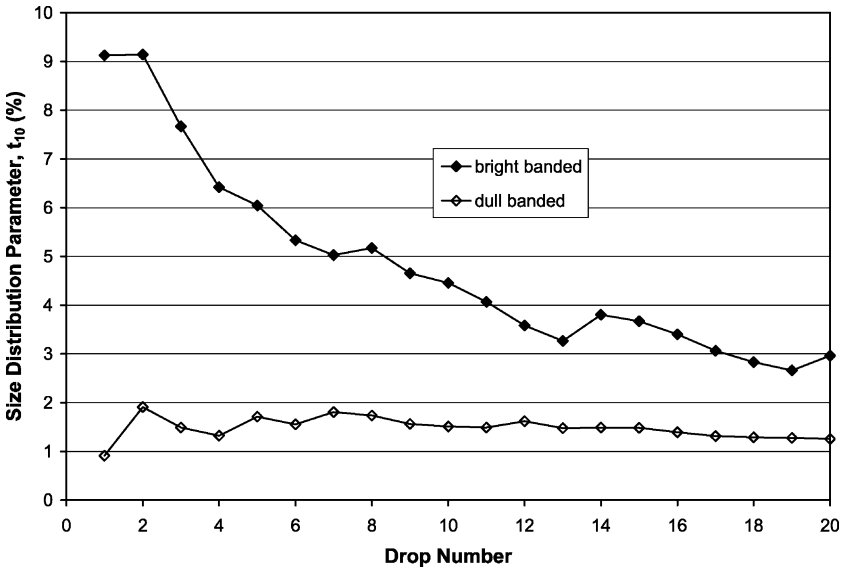

Fig. 6. Conditioning test results for banded-bright and dull-banded coal from study seam.

coal texture arising from cleats and band contacts after the first few drops.

The dull banded coal displays a very different breakage behaviour to bright banded coal. The t10 parameter remains constant (1–2%) for every drop. There is no hardening effect as seen in the banded-bright coal. This is due to the dull-banded coal's sparsity of cleating and low flaw density. During the breakage process, the dull particles survive as large particles relative to their starting size, with just their corners gradually being knocked off by attrition. This breakage mechanism creates a constant amount of fines after each drop. An important point to note for both coal types is that breakage does not stop, even after 20 drops. The breakage mechanisms and rates of each coal type may be different, but breakage will still occur after a large number of drops.

In summary, increasing energy results in increased size reduction. The brighter the particle, or the larger the particle, the greater the size reduction for a given energy. Hence, thick layers of friable banded-bright and inter-banded coal should reduce to their component bands more readily than will harder duller coals, which already exist as relatively massive, or texturally homogeneous entities. As a result, the melange of different components participating in the drop-shatter process begins to reach an equilibrium, or fatal size distribution. Based on the drop-shatter tests, this occurs early in the process and at relatively low energies.

4.4. Drop-shatter sizing results

The results of the drop-shatter tests also demonstrate that size reduction increases with increasing energy due to the number of drops. The intact core (that was 100% recovered) is assumed to have experienced zero breakage in the ground. However, sizing the material prior to testing suggested that some breakage occurred during transport from field to laboratory. Material loss during the testing was minimal, as demonstrated in Table 3.

The graph in Fig. 7a presents the drop-shatter results for the 100 mm core as a fineness indicator, here the mass percent passing 2 mm, against the number of drops and their equivalent impact energy. Similar to the drop weight results, the rate of breakage is rapid in the first four to six drops, or approximately 0.025 kW h/t, thereafter declining slightly.

The effect of bulk ply composition is observed in the results. The basal Ply C, which contains the most banded-bright coal, is the most friable of the plies, followed closely by the top Ply A, then the middle Ply

Table 3
Mass of plies prior to and after 20 drops in the drop-shatter process

	Ply A	Ply B	Ply C
Mass before drop shattering (kg)	23.4	50.3	12.8
Mass after drop shattering (kg)	22.6	49.6	12.4
Mass prior to progeny analysis (kg)	22.6	49.4	12.4

B that contains the most dull lithotypes. If an arbitrary target size of 30% passing 2 mm was chosen, the brightest Ply C would achieve this at a lower energy, around 12 drops or 0.065 kW h/t, than would the hardest middle Ply B at 20 drops, or 0.1 kW h/t.

Cores extracted at 1 m intervals adjacent to the study core confirm the differing breakage behaviours

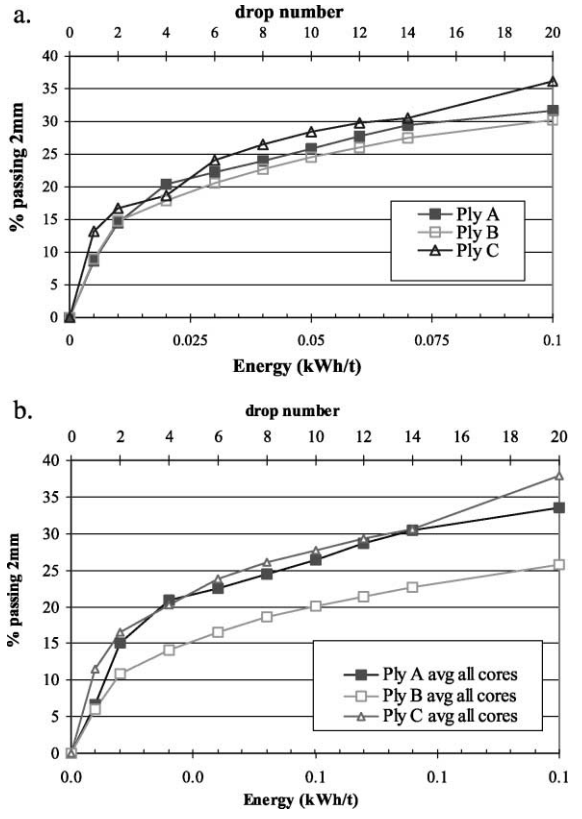

Fig. 7. Drop-shatter results for each ply displayed as a fineness indicator, percent passing 2 mm, for increasing number of drops. Equivalent energies are displayed on the lower *x*-axis. (a) Results for 100 m core, (b) results averaged for 63, 100 and 200 mm cores.

Table 4
Percent passing 2 mm for drop-shatter products from initial sizing to 20 drops for three adjacent cores demonstrating standard deviations

	Core/drop number								
	Initial	2	4	6	8	10	12	14	20
Ply A									
Slim core	8.35	14.39	17.87	20.58	21.95	24.03	26.60	28.84	33.76
100 mm	8.66	14.47	23.64	22.24	23.95	25.83	27.76	29.44	31.66
200 mm	2.78	16.38	21.20	24.71	27.27	29.53	31.48	33.15	34.99
Ply A avg	6.60	15.08	20.90	22.51	24.39	26.46	28.61	30.48	33.47
STD	3.31	1.13	2.90	2.08	2.69	2.81	2.55	2.33	1.69
Ply B									
Slim core	5.89	9.59	12.33	14.10	16.15	16.87	17.92	18.92	22.39
100 mm	8.95	14.78	17.89	20.57	22.69	24.55	26.01	27.49	30.24
200 mm	3.24	8.41	12.24	14.76	16.84	18.80	20.13	21.69	24.69
Ply B avg	6.03	10.93	14.15	16.47	18.56	20.07	21.35	22.70	25.77
STD	2.86	3.39	3.24	3.56	3.59	3.99	4.18	4.37	4.03
Ply C									
Slim core	15.19	18.65	21.96	22.94	24.12	24.88	26.06	26.99	34.39
100 mm	13.17	16.71	18.66	24.08	26.48	28.41	29.78	30.53	36.15
200 mm	5.93	14.44	20.27	24.48	27.50	29.91	32.05	34.11	43.26
Ply C avg	11.43	16.60	20.30	23.83	26.03	27.73	29.30	30.54	37.93
STD	4.87	2.11	1.65	0.80	1.74	2.59	3.02	3.56	4.70

of the different plies (Table 4 and Fig. 7b; data from Esterle et al., 2000b). Little data are available in the public domain to test the reproducibility of the drop-shatter test, basically because of the expense of coring and testing, and there is always inherent variability between even closely spaced cores (Swanson et al., 1998). Nevertheless, the results of closely spaced, but different diameter (63, 100 and 200 mm) cores from the same seam suggest that differences greater than 5% should be significant. On average, the basal Ply C, which contains the most banded-bright coal, is the most friable of the plies, followed by the top and middle Plies A and B, respectively.

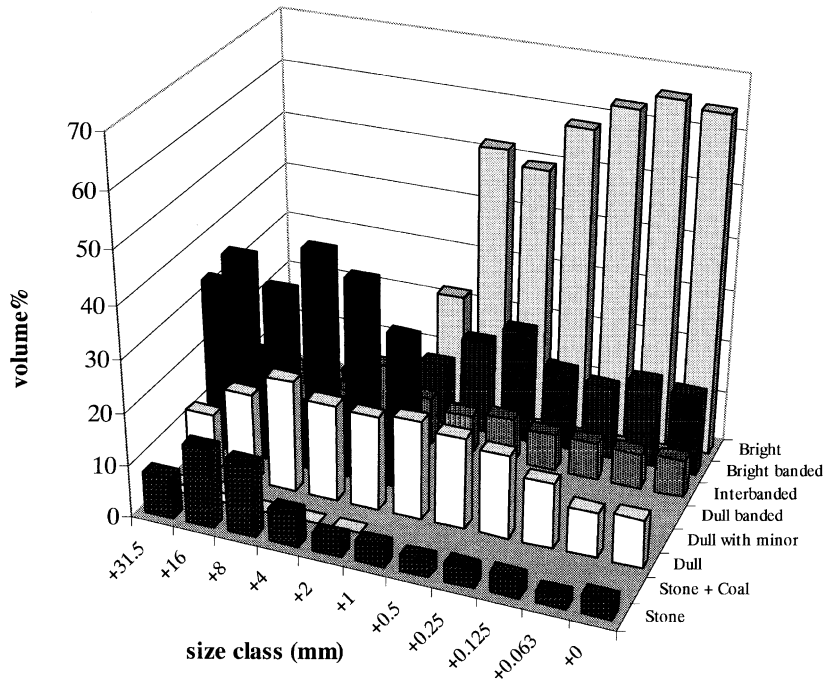

Fig. 8. Proportion of lithotypes in each size classes of daughter particles after 20 drops, composite of total core. Each size class adds to 100%.

4.5. Composition of the daughter particles after drop-shatter

The composition of the daughter particle size fractions was used to determine (1) the composition of the plies and composite core, relative to that estimated by profiling and (2) the relative size distribution of the different components after 20 drops in the drop-shatter process. Although an arbitrary end to the process, breakage rates have declined significantly by 20 drops and the daughter particle size distribution can be considered as relatively stable.

The composition of each size fraction is presented in Fig. 8. To be consistent with the microscopic data, the mass in each fraction was converted to volume. Data as mass, volume and frequency are given in Appendix A, Tables A-5 to A-8, and they show little difference in estimating the composition of the broken particle size fractions. The bright and banded-bright lithotypes dominate the fine sizes less than 1 mm in the broken daughter particles. The total proportion of inter-banded coal is low and is distributed across the size ranges. Dull coal, mixed stone and coal, and stone dominates the coarser size fractions greater than 1 mm. The absence of material in the 2 + 1 mm size fraction was not a function of the change in the characterisation

Table 5
Composition of plies and composite seam estimated from lithotype and band profiles and from daughter particles resulting from drop-shatter test (data from Kolatschek, 2000)

	Proportions	Lithotype (vol.%)	Band (vol.%)	Daughter (vol. %)
Ply A	Bright (%)	37.79	37.42	37.2
	Dull (%)	55.07	52.34	53.04
	Stone (%)	7.14	10.23	9.72
Ply B	Bright (%)	19.13	22.35	22.4
	Dull (%)	65.04	61.56	62.93
	Stone (%)	15.83	16.1	14.68
Ply C	Bright (%)	52.85	48.02	42.05
	Dull (%)	43.01	48.73	51.75
	Stone (%)	4.15	3.24	6.2
Total core	Bright (%)	32.51	32.62	29.26
	Dull (%)	56.91	55.94	58.64
	Stone (%)	10.58	11.44	12.1

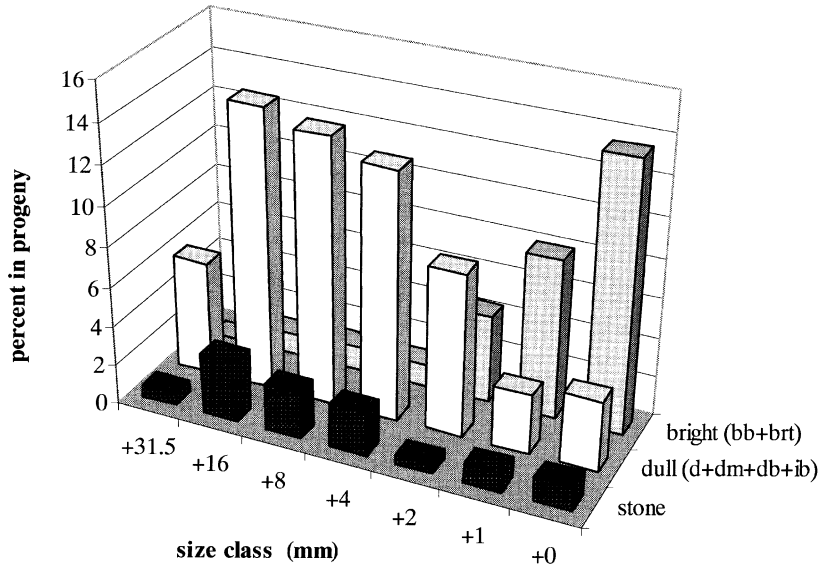

Fig. 9. Size distribution of end-member bright, dull and stone categories across all daughter particles.

methods, as was verified by examining size fractions between 4 and 0.5 mm by both megascopic and microscopic methods.

Characterisation of the daughter particles suggested that the output composition could be easily described by a ternary system of bright and dull coal and stone. As a result, the data were grouped into their end-member categories of bright, dull and stone for further analysis. The grouped compositions of the daughter particles and intact core samples are compared in Table 5. The reconciliation between the compositions estimated by lithotype and band profiling, and daughter particle characterisation, is good for both the plies and the total core, verifying that all components were accounted for during characterisation.

The next step was to examine the changes in the size distribution of the different end-member components. The proportion of end-member components in each size fraction was normalised across the total core using the mass distribution of size fractions obtained from the sieve analysis after 20 drops. The resulting distribution is shown in Fig. 9. Stone particles are predominantly coarse, occurring in the 32 + 16 mm size fraction. Dull coal is also coarse, occurring in the 32 to 4 mm size fractions. Bright coal is fine and dominates the < 2 mm fractions.

4.6. Comparison of parent and daughter particle size distributions

In order to test the hypothesis that the daughter particle size and composition is relational to the parent stratigraphy, the thickness distributions of the lithotypes and bands were compared to the size distribution of the broken daughter particles after the series of

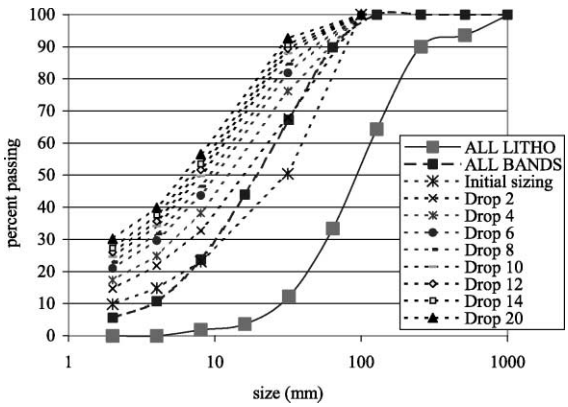

Fig. 10. Comparison of lithotype and band thickness distributions, weighted by mass, with daughter particle size distributions from the drop-shatter process.

drops out to 20. The calculated mass distributions of all lithotypes and all bands (regardless of type) are compared to the daughter particle distributions in Fig. 10. This comparison suggests that breakage and size reduction occur very early in the process and, in fact, that the component bands are liberated before the drop-shatter process even begins. The component bands then continue to break down out to 20 drops. Physically, this scenario is difficult to believe as one can see composite lithotypes in the daughter particles after two drops.

The size distributions of the daughter particles are compared to the lithotype and band frequency distributions in Fig. 11. In this scenario, the intact lithotype and band distributions envelope the breakage process from initial sizing out to 20 drops, and suggest that the component bands approach liberation from the parents. This scenario more closely matches the distribution of the lithotypes as found by the daughter particle characterisation. Based on this, the frequency distributions of the end-member lithotypes and bands were compared to the size distributions of bright and dull coal and stone (Figs. 12–14).

The frequency distributions of the bright and dull bands match well with the size distribution of liberated bright and dull coal estimated from the broken daughter particles. Stone is a little more variable. The greatest amount of fragmentation and size reduction from lithotype to band occurred in the end-member bright coal category, which is the most friable due to the abundance of thin to thick vitrain bands with tightly spaced cleat. Size reduction also occurred, but to a lesser extent, within the dull lithotype, as this coal type is harder and contains sparser and more widely spaced cleat. This was also observed in the conditioning experiment.

The results suggest that the individual components are liberated during the breakage process, and their inherent thickness distribution will estimate a relatively stable and final size distribution. This suggests that Ferm's hypothesis was correct, and that the parent stratigraphy, or the thickness distribution of the hardest

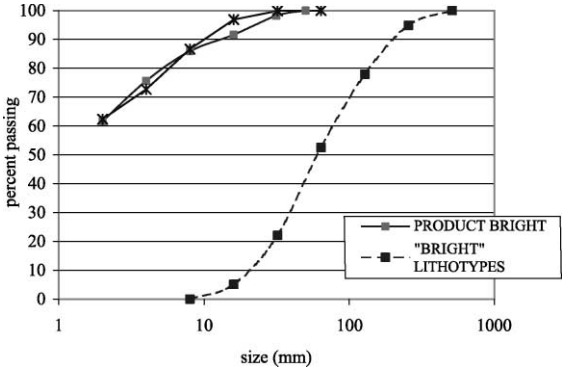

Fig. 12. Comparison of bright lithotype and band thickness distributions with size distribution of bright coal in daughter particles after 20 drops.

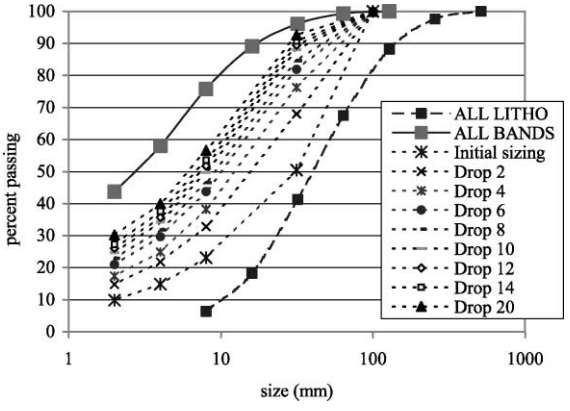

Fig. 11. Comparison of lithotype and band thickness distributions, as frequency, with daughter particle size distributions from the drop-shatter process.

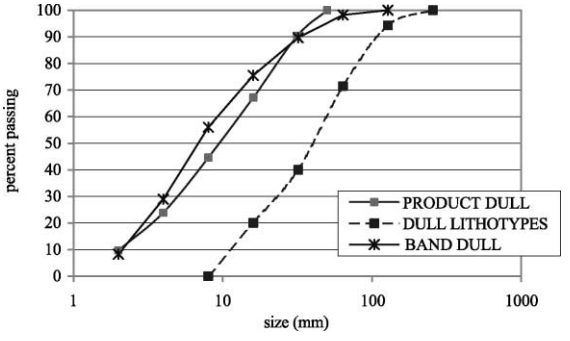

Fig. 13. Comparison of dull lithotype and band thickness distributions with size distribution of dull coal in daughter particles after 20 drops.

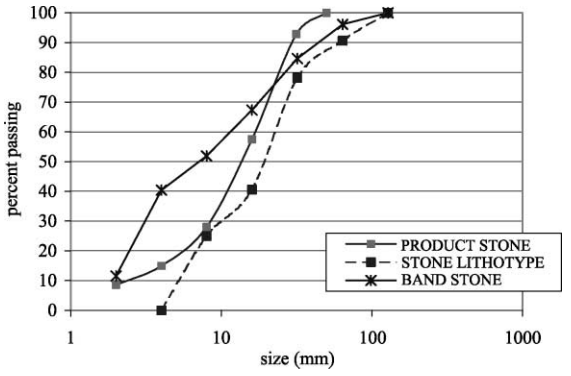

Fig. 14. Comparison of stone band thickness distributions measured during lithotype and band profiling, with size distribution of stone in daughter particles after 20 drops.

and softest components within a seam, can be used to estimate not only the composition of daughter particles, but also their size distribution. Dull bands start big, and stay big. Bright bands start small, but usually occur in thicker composites that break easily and rapidly down to a size relative to the component band thickness. The most significant size reduction occurs within the first two to four drops, equivalent to an energy of 0.01–0.02 kW h/t. Thereafter, the amount of breakage declines with each successive drop. However, the process never completely stops and more energy is required to liberate all bands within the seam.

5. Empirical description of the breakage process

During fragmentation from the in situ coal mass, the lithotypes disseminate into their end-member band components bright, dull and stone. The rate of breakage is rapid in the first few drops, thereafter declining, but continuing. In the Permian-age coals examined by the authors in Australia, dull bands are inherently thicker than bright bands within lithotypes for a given seam. The inherent coarseness, when combined with hardness, results in the tendency for coarser size fractions to be dominated by dull coal and stone. The more friable, brighter coal lithotypes will break down into finer fractions more readily, resulting in their concentration in the fines (McCabe, 1942). This was corroborated by the characterisation work conducted on the progeny after the final 20 drops in the process.

One of the objectives of this project was to determine whether these differences in coal hardness and texture observed in situ in a coal seam could be used to predict the resulting size distributions after drop-shatter. Although it is not a one to one comparison, the relative differences in size distributions are retained throughout the process.

The "fatal size" distribution, described earlier, suggests that coals reach equilibrium during the breakage process where the rate of breakage declines as a function of the different components. Brighter coals break to smaller particles faster than duller particles and stone; as smaller particles require more energy for breakage, the process is self-limiting and the rates of breakage for the components converge.

6. Implications for mining and processing

The preliminary design of mining and coal processing methods and the selection of appropriate equipment hinge on the character of the coal. Bore cores are an integral part of the evaluation process and they provide data regarding the size of the coal reserve, the mining conditions, the coal quality and its processing characteristics. The processing characteristics are commonly obtained through drop-shatter testing (often combined with wet tumbling) and washability analysis of the resulting daughter particles.

Very simply described, coal processing is a size by density operation. Therefore, poor estimations of particle size distribution that will report to a plant will reduce the efficiency of the plant circuits or result in expensive retro-fitting after operations have begun. Fine coal, that is <0.5 mm wedge wire, is a particular problem, even though modern flotation cells have increased the efficiency and reduced the costs of processing fines. Fine coal is difficult to transport, expensive to clean and dewater and therefore leads to higher costs. On the other hand, fine coal (including slightly coarser particles up to 2 mm) is well liberated with respect to bright, or vitrinite maceral content and mineral matter, adding to product value for coking coals in Australian Permian coals (Nicol, 1992). Predicting the particle size and product character correctly will increase the efficiency and profitability of the

operations, and these two properties are directly related to the inherent rank and parent stratigraphy of the coal, and to the energy exerted on the coal during the mining and handling operations. If the results of this study are transferable to other seams, in particular seams with very different brightness profiles, than one can start to estimate size and composition from the frequency distributions of the bright, dull and stone bands. Add density and mineral matter liberation, then one can predict washability. These data can be routinely collected during exploration and subsequent drilling phases at any mine site.

In an operational sense, the banded-bright coal requires substantially less energy than does the dull coal for fragmentation and liberation of the stone from coal. This can impact blast design and positioning of the charge, where the objective is to fragment the coal for efficient loading without producing excessive fines. In thick seams that exhibit ''dulling up'' trends, there is a trade-off between loosening the toe for load shovel productivity and increasing the tonnages in the fines circuits, resulting in higher processing costs compared to cleaning coarse coal. It has also been suggested that blast design can assist in improving mineral matter liberation, in addition to fragmentation by focusing the blast energy in the duller, stone band-rich coals (Esterle et al., 2000a,b). Vertical variation in coal fragmentation behaviour is also an issue for selective mining and its impact on downstream processing. This is of particular concern in Queensland, Australia, where some open cut mines extracting thick (>4.5 m) seams have reached their overburden ratio limits and will change to high wall, auger or long wall mining methods in which the lower, generally banded-bright portions of the seams are selectively extracted.

7. Conclusions

The breakage process in coal is a function of the amount of energy imparted to the material and the inherent strength or friability of the material. For a given energy, banded-bright coals produce more fine particles than do dull coals and stone. Smaller block sizes require more energy to break to a given proportion of their top size. The inherent lithotype thickness distribution is coarser for banded-bright to interbanded coal types, but these composites consist of thinner bands of bright and dull coal. As they require less energy to fragment and liberate their component bands, they reduce quickly during the breakage process. The component dull bands in coal then start to dominate the coarser size fractions, but they require more energy to break, regardless of size. As a result, the coal becomes ''conditioned'' during breakage as particles reach equilibrium. This results in a ''fatal size'' distribution, beyond which coals require more energy than can be achieved by breakage to increase their rate of size degradation.

The parent stratigraphy of a coal seam, as measured by lithotype and band profiling, provides an estimate of the size reduction that occurs during the process. After coals approach or surpass their fatal size, they can be considered a ternary system of bright (soft) and dull (hard) coal and, in this case, hard stone. As a result, dull coals tend to dominate the coarser size fractions of the broken particles whereas bright coals dominate the fines. Based on the frequency distributions, one can estimate the daughter particle size distributions of the end-member components, as well as their composition.

Acknowledgements

This idea started when John Ferm took an interest in coal and peat texture in the mid-1980s starting with Tim Moore and Indonesian coal. Besides ''just being neat'', John could see the industrial applications that textural analysis might have, and a number of his students had to chase it. Funding for this study came through a much larger project examining fundamental and operational controls on coal fragmentation and fines generation through the Australian Coal Association Research Programme (ACARP Project C6046), the Centre for Mining Technology and Equipment and BHP Coal Australia. Yvonne Kolatschek, as part of a MSc thesis, collected data. Candid and constructive reviews were conducted by Drs. Zhu Rui and Hakan Kahraman of the CSIRO, Mr. Dick Sanders of Quality Coal Consulting in Australia, and by Dr. Jim Hower of the Kentucky Center for Applied Energy Research and an anonymous reviewer. We thank them. It's now up to someone else to test the hypothesis, particularly in seams of different ages and character.

Appendix A

Table A-1. Density measurements by lithotype, Ply A

Size fraction (mm)	Density (g/cm^3)						
	ST	D	DMB	DB	IB	BB	B
+31.5	2.15	1.73	1.41	1.42	1.33	1.35	1.34
31.5+16	2.38	1.68	1.48	1.45	1.42	1.35	1.34
16+8	2.49	1.48	1.42	1.39	1.34	1.32	1.31
8+4	2.39	1.63	1.52	1.41	1.34	1.32	1.31
4+2	2.36	1.64	1.42	1.36	1.31	1.31	1.27
−2	2.36	1.64				1.31	1.27

Table A-2. Density measurements by lithotype, Ply B

Size fraction (mm)	Density (g/cm^3)						
	ST	D	DMB	DB	IB	BB	B
+31.5	2.41	1.79	1.45	1.41	1.38	1.37	1.33
31.5+16	2.20	1.67	1.51	1.43	1.36	1.37	1.33
16+8	2.39	1.62	1.46	1.43	1.35	1.34	1.30
8+4	2.40	1.60	1.47	1.38	1.34	1.34	1.30
4+2	2.44	1.60	1.36	1.34	1.33	1.33	1.29
−2	2.44	1.60				1.33	1.29

Table A-3. Density measurements by lithotype, Ply C

Size fraction (mm)	Density (g/cm^3)						
	ST	D	DMB	DB	IB	BB	B
+31.5	2.38	1.41	1.41	1.36	1.34	1.31	1.31
31.5+16	2.33	1.41	1.41	1.35	1.32	1.29	1.29
16+8	2.25	1.44	1.39	1.37	1.32	1.31	1.31
8+4	2.42	1.53	1.45	1.35	1.31	1.31	1.31
4+2	2.46	1.49	1.39	1.32	1.30	1.30	1.26
−2	2.46	1.49				1.30	1.26

Table A-4. Averaged density measurements for lithotypes across all sizes and plies

Size fraction (mm)	Density (g/cm^3)						
	ST	D	DMB	DB	IB	BB	B
Average all sizes	2.37	1.58	1.44	1.38	1.34	1.33	1.30

Table A-5. Mass composition for daughter particles, total core

Lithotype	Size fraction (mm)				
	+31.5	31.5+16	16+8	8+4	4+2
	Mass%				
Stone	11.74	21.11	20.84	9.90	5.89
Stone+coal	1.88	2.19	0.15	0.07	0.00
Dull	12.90	17.53	21.14	19.52	19.88
Dull with minor	30.92	19.24	10.69	13.90	10.08
Dull-banded	31.98	26.33	34.37	32.02	23.83
Inter-banded	10.14	8.58	6.47	12.76	8.71
Banded-bright	0.45	5.02	6.13	9.04	11.30
Bright	0.00	0.00	0.22	2.80	20.31
Total	100.00	100.00	100.00	100.00	100.00

Table A-6. Frequency composition for daughter particles, total core

Lithotype	Size fraction (mm)				
	+31.5	31.5+16	16+8	8+4	4+2
	Frequency%				
Stone	9.31	14.99	15.01	6.84	3.17
Stone+coal	2.51	1.63	0.04	0.09	0.00
Dull	12.42	18.43	22.21	19.25	18.50
Dull with minor	23.69	20.40	10.04	12.27	8.58
Dull-banded	34.00	28.48	36.69	33.06	22.77
Inter-banded	16.66	9.99	7.97	13.31	9.14
Banded-bright	1.41	6.08	7.77	10.95	12.87
Bright	0.00	0.00	0.27	4.23	24.95
Total	100.00	100.00	100.00	100.00	100.00
Total number of particles	81	1678	1755	2952	2838
Mass of particles counted (g)	5361.86	15,375.89	1821.80	369.20	41.50
Total mass of fraction (g)	5395.86	15,478.00	14,352.89	13,360.44	11,110.60

Table A-7. Volumetric composition for daughter particles, total core

Lithotype	Size fraction (mm)				
	+31.5	31.5+16	16+8	8+4	4+2
	Vol.%				
Stone	7.92	15.07	13.86	6.28	3.51
Stone+coal	1.43	1.83	0.11	0.05	0.00
Dull	11.54	17.09	21.38	18.53	17.92

Table A-7 (*continued*)

Lithotype	Size fraction (mm)				
	+31.5	31.5+16	16+8	8+4	4+2
	Vol.%				
Dull with minor	32.83	20.68	11.75	13.99	10.44
Dull-banded	34.41	29.41	38.38	34.24	25.03
Inter-banded	11.40	9.99	7.34	13.98	9.24
Banded-bright	0.48	5.93	6.95	9.85	11.93
Bright	0.00	0.00	0.24	3.08	21.94
Total	100.00	100.00	100.00	100.00	100.00

Table A-8. Results of microscopic analysis for daughter particles, total core

Lithotype	Size fraction (mm)					
	2+1	1+0.5	0.5+0.25	0.25+0.125	0.125+0.063	−0.063
	Count%					
Bright	52.00	49.41	58.30	63.07	65.74	64.52
Banded-bright	17.90	21.59	15.32	13.88	16.49	15.56
Inter-banded	7.38	8.41	7.03	7.06	6.76	7.13
Low ash dull	14.19	10.00	11.19	9.73	6.57	7.58
High ash dull	4.59	7.40	4.68	2.59	2.21	1.69
Stone	3.94	3.18	3.47	3.68	2.24	3.52
Total	100.00	100.00	100.00	100.00	100.00	100.00

References

American Society for Testing and Materials, 1986. D440-86 (reapproved 1994), Standard method of drop-shatter for coal. Am. Soc. Test. Mater., Philadelphia, USA.

Bailey, J.G., Esterle, J.S., 1996. Application of coal textural analysis to predict grinding behaviour and product composition in Australian coals. ACARP Final Report Project No. 940083, 32 pp.

Diessel, C.F.K., 1965. Correlation of macro- and micro-petrography of some New South Wales coals. 8th Commonwealth Mining and Metallurgy Congr., Melbourne, Australia, 1965. Australian Inst. Mining Metall., Melbourne, pp. 669–677.

Esterle, J.S., O'Brien, G., Kojovic, T., 1994. Influence of coal texture and rank on breakage energy and resulting size distributions in Australian coals. 6th Australian Coal Science Conference; Newcastle, Australia, 1994. Australian Inst. Energy, Newcastle, pp. 175–181.

Esterle, J., Kanchibotla, S.S., Thornton, D., 2000a. Using brightness profiles to optimise coal blasting. In: Beeston, J.W. (Ed.), Bowen Basin Symposium 2000 — The New Millenium, Geol. Soc. Australia, Coal Geology Group and The Bowen Basin Coal Geology Group, Rockhampton, Oct 2000, pp. 181–190.

Esterle, J.S., Thornton, D., O'Brien, G., Kojovic, T., Cocker, A., 2000b. Optimising fragmentation for improved recovery, ACARP C6046 Final Report, 269 pp.

Hower, J.C., 1998. Inter-relationship of coal grinding properties and coal petrology. Min. Metall. Proc. 15 (3), 1–16.

Hunt, J.W., 1988. Sedimentation rates and coal formation in the Permian basins of Eastern Australia. Aust. J. Earth Sci. 35 (2), 259–274.

Kolatschek, Y., 2000. Modelling the drop-shatter process using lithotype description and single particle breakage results. Unpublished MSc thesis, University Of Queensland, 269 pp.

McCabe, L.C., 1942. Practical significance of the physical constitution of coal in coal preparation. J. Geol. 2, 406–410.

Moore, T.A., Ferm, J.C., 1988. A modification of procedures for petrographic analysis of Tertiary Indonesian coals. J. Southeast Asian Earth Sci. 2, 175–183.

Moore, T.A., Ferm, J.C., 1992. Composition and grain size of an

Eocene coal bed in southeastern Kalimantan, Indonesia. Int. J. Coal Geol. 21 (1–2), 1–30.

Moore, T.A., Hilbert, R.E., 1992. Petrographic and anatomical characteristics of plant material from two peat deposits of Holocene and Miocene Age, Kalimantan, Indonesia. Rev. Palaeobot. Palynol. 72 (3–4), 199–227.

Narayanan, S.S., Whiten, W.J., 1988. Determination of comminution characteristics from single-particle breakage tests and its application to ball-mill scale-up. Trans. Inst. Min. Metall. 97, C115–C124.

Nicol, S.K., 1992. Fine coal beneficiationSwanson, A.R., Partridge, A.C. (Eds.), Adv. Coal Prep. Monogr. Ser., Australian Coal Prep. Soc. 4 (9) 181 pp.

Rittenger, V.R.P., 1867. Textbook of Mineral Dressing. Ernst und Korn, Berlin, Germany.

Schopf, J.M., 1960. Field description and sampling of coal beds. Geol. Surv. Bull. 1111-B 67 pp.

Shearer, J.C., Moore, T.A., 1994a. Grain-size and botanical analysis of two coal beds from The South Island Of New Zealand. Rev. Palaeobot. Palynol. 80 (1–2), 85–114.

Shearer, J.C., Moore, T.A., 1994b. Botanical control on banding character in two New Zealand coal beds. Palaeogeogr., Palaeoclim., Palaeoecol. 110 (1–2), 11–27.

Shearer, J.C., Moore, T.A., Demchuk, T.D., 1995. Delineation of the distinctive nature of Tertiary coal beds. In: Demchuk, T.D., et al. (Eds.), Tertiary-Age Coals, GSA Symposia. Int. J. Coal Geol. 28 (2–4), 71–98.

Smyth, M., Cook, A.C., 1976. Sequence in Australian coal seams. Math. Geol. 8 (5), 529–547.

Standards Association of Australia, 1993. AS 2519-1993. Guide to the technical evaluation of higher rank coal deposits. Sydney, Australia.

Standards Association of Australia, 1994. AS 1038.21.1,1-1994. Coal and coke-analysis and testing. Part 21.1.1, Higher rank and coke-relative density-analysis sample/density bottle method. Sydney, Australia.

Stopes, M.C., 1919. On the four visible ingredients in banded bituminous coals. Proc. R. Soc., Ser. B 90, 497–508.

Swanson, A.R., Fletcher, I.S., Partridge, A.C., 1993. Improved prediction of size distributions and their effects in materials handling and coal preparation systems, Final Report for NERDDC Project 1290.

Swanson, A.R., Fletcher, I.S., Membrey, W., Davis, R., 1998. Improved washability prediction through establishment of correct coal size distributions. Final Report for ACARP Project No. C5053.

Wang, Z., Hower, J.C., Ferm, J.C., Wild, G.D., 1996. Characteristics of lithotype thickness and sequential association of some Kentucky coals. Org. Geochem. 24 (2), 189–195.

Ward, S.D., Moore, T.A., Newman, J., 1995. Floral assemblage of the “D” coal seam (Cretaceous): implications for banding characteristics in New Zealand coal seams. N. Z. J. Geol. Geophys. 38 (3), 283–297.